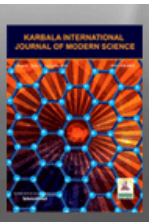

Karbala International Journal of Modern Science

Volume 6 | Issue 2 Article 5

Preparation of Glass Ionomer Cement from Recycled Low Alumina Glass

Sura S. Al-Tae'e
Department of Materials Engineering - University of Technology - Iraq, 130016@uotechnology.edu.iq

Ola M. Almitwalli
Department of Materials Engineering/ University of Technology, Iraq, olam.almitwalli@gmail.com

Saad B. H. Farid
Department of Materials Engineering/ University of Technology, Iraq, Dr.SaadBHF@gmail.com

Recommended Citation

Al-Tae'e, Sura S.; Almitwalli, Ola M.; and Farid, Saad B. H. (2020) "Preparation of Glass Ionomer Cement from Recycled Low Alumina Glass," *Karbala International Journal of Modern Science*: Vol. 6 : Iss. 2 , Article 5.
Available at: https://doi.org/10.33640/2405-609X.1410

Preparation of Glass Ionomer Cement from Recycled Low Alumina Glass

Abstract

Fluoroaluminosilicate glass was prepared from recycled low alumina glass, with the additions of AlF_3 and CaF. That was to provide a cheap source of proper glass required to prepare glass ionomer cement GIC. Three batches of the fluoroaluminosilicate glass were prepared with different additions of CaF varied at the expense of AlF_3. i.e., the glass was prepared with three different CaO contents. The prepared glasses were used as an essential part of GICs. It was found that a crystalline phase (fluorapatite) appeared as part of the set cement matrix. The XRD of the set cements indicated that the crystalline fluorapatite increases with the increase of the CaO content of the starting fluoroaluminosilicate glass. The increase of the CaO content also led to an increase in the density of the set cement and its compressive strength. In addition, the working and setting times were increased too. Finally, the set cements where shown bioactive.

Keywords

GIC; Recycled materials; Low alumina glass; Fluorapatite; Bioactivity

1. Introduction

Glass Ionomer Cement (GIC) is essentially an aluminosilicate glass particulates that reacted with a polymeric acid. The acid should be water-soluble and the glass composition should be basic. That is, the acid reacts with a part of the glass particulates forming a gel phase. A paste of high viscosity is produced that gradually sets in minutes to give enough working time; i.e. an adequate time for paste manipulation and shaping. When the viscosity of the paste is too high for further manipulation, the setting time is reached. Finally, the reaction yields a solid composite of the gel matrix with glass particulates as reinforcement; i.e. a set cement. The composition of the aluminosilicate glass also includes calcium and sodium to maintain its basic character. The phosphate may be added to the composition to enhance the formation of the glass network via reaction with aluminum. Moreover, fluoride is added to the composition to decrease the melting temperature of the glass batch and to gain the benefit of the fluoride release of the set cement. In that case, fluoroaluminosilicate glass is obtained. The fluoride release takes place in acidic conditions, thus, neutralizing the surrounding medium that protects from tooth decay and dental caries. The translucency and strength of the set cement were also shown to be improved by the existence of the fluoride. Other additives were found of high benefits such as tartaric acid, which prevents early cross-linking by forming a water-soluble complex. This delay of the cross-linking provides extra working time for the cement [1,2].

The fluoroaluminosilicate glass compositions required for the GIC may be bounded by the following range in w.t.%: SiO_2 24.9−30.1, Al_2O_3 14.2−19.9, AlF_3 0.-4.6, CaF_2 12.8−34.5, $NaAlF_6$ 0.-19.2, NaF 0.-3.7, $AlPO_2$ 0.0−24.2 [1−4]. Yet, very educational articles in the design of the GIC can be found in Ref. [5−9]. The composition of the acidic part of the cement is out of the scope of this work. However, the acidic part is fairly discussed in Refs. [1−4,10], particularly, in Ref. [4].

Numerous studies have been focused on the composition of the solid part with two strategies. The first is to study the effect of additives to the fluoroaluminosilicate glass to promote their mechanical properties; such as the addition of Nano-clays [11,12], Zirconia and alumina [13,14]. Also, to enhance both mechanical and remineralizing properties via the addition of hydroxyapatite [15−18], bioactive glass [19], TiO_2 nanotubes [20], E-glass fibers [21], fluorinated graphene [22], and cellulose nanocrystals [23]. A summary of these and other fillers can be found in Ref. [24]. The second strategy is the modifications to the chemical composition of the fluoroaluminosilicate glass, e.g. incorporation of ZnO and MgO as a replacement for CaO [25]. The above-mentioned modification of the GIC also affects their working and setting times. Comprehensive reviews for the effect of the modifications of the GIC's to their properties is the subject of many recent articles [26−31].

In this work, simple and cheaper compositions of GIC's were prepared. The compositions were based on recycled low alumina glass with the addition of AlF_3 and CaF. The CaF is varied at the expense of AlF_3 in these compositions and the resultant glass properties were compared.

2. Materials and methods

The starting materials were a recycled low alumina glass, aluminum fluoride AlF_3, calcium fluoride CaF, and phosphoric acid H_3PO_4. The chemical composition of the utilized low alumina glass is shown in Table 1. Calculated amounts of the starting materials were utilized to obtain the target composition of three batches of the fluoroaluminosilicate glass shown in Table 2. The chosen compositions shown in Table 2 is designed so that the calcia increase in the step of 5 w.t.% at the expense alumina. The 'rem' is the w.t.% of the remaining materials in the utilized low alumina glass excluding silica, alumina, and calcia.

The low alumina glass was crushed and milled to reach a submicron average particle size. The P_2O_5

Table 1
The composition in w.t.% of the low alumina glass.

SiO_2	Al_2O_3	CaO	Na_2O
72.69	1.45	5.01	16.43
K_2O	MgO	Fe_2O_3	TiO_2
0.35	3.46	0.60	0.01

Table 2
The composition in w.t.% of the obtained fluoroaluminosilicate glass.

Batch	SiO_2	Al_2O_3	CaO	F	P_2O_5	rem
#1	30.0	24.4	7.07	15.33	14.60	8.6
#2	30.0	21.9	9.57	14.78	15.14	8.6
#3	30.0	19.4	12.07	14.23	15.69	8.6

https://doi.org/10.33640/2405-609X.1410

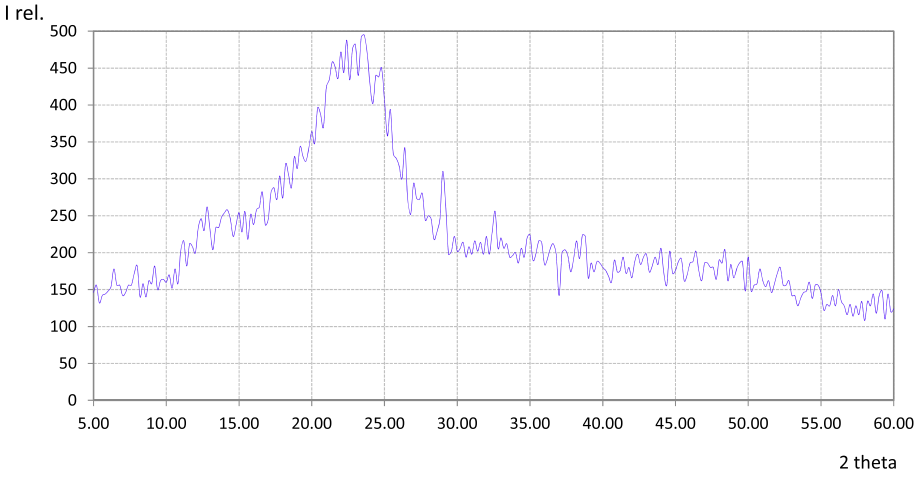

Fig. 1. X-ray diffraction pattern of the prepared fluoroaluminosilicate glass.

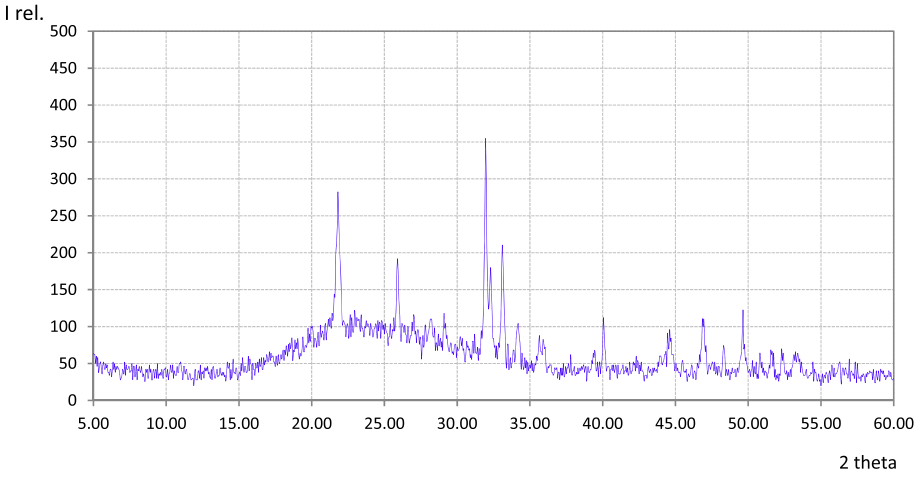

Fig. 2. X-ray diffraction pattern for the set cement #1.

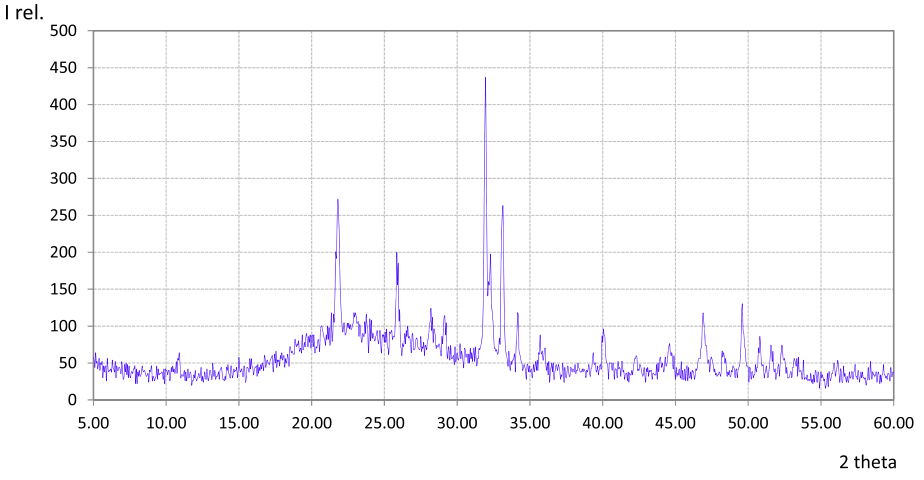

Fig. 3. X-ray diffraction pattern for the set cement #2.

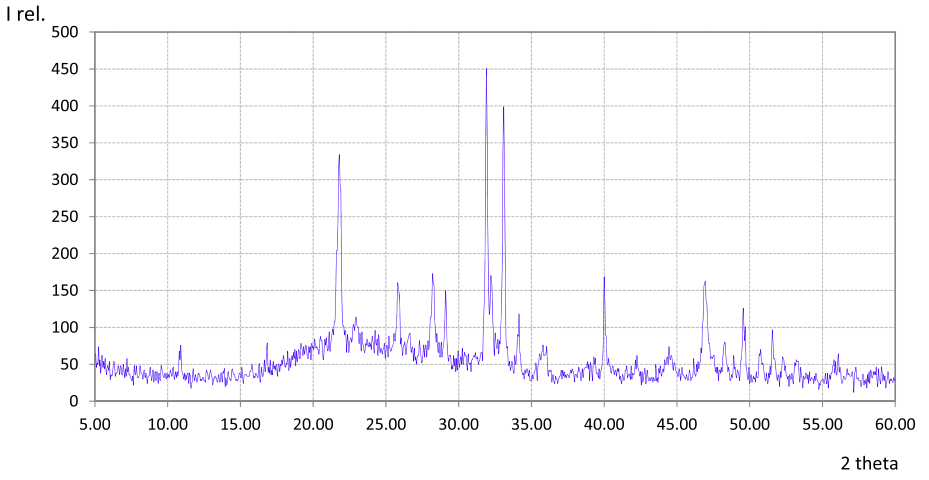

Fig. 4. X-ray diffraction pattern for the set cement #3.

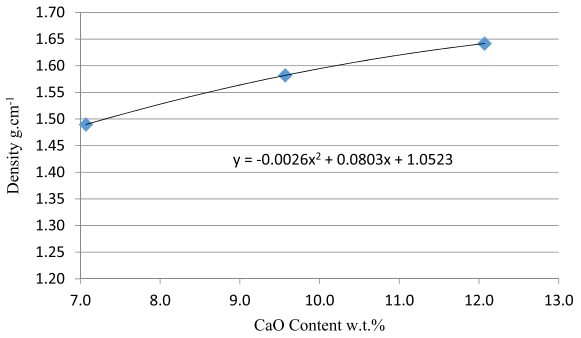

Fig. 5. Density of the set cements as a function of CaO content.

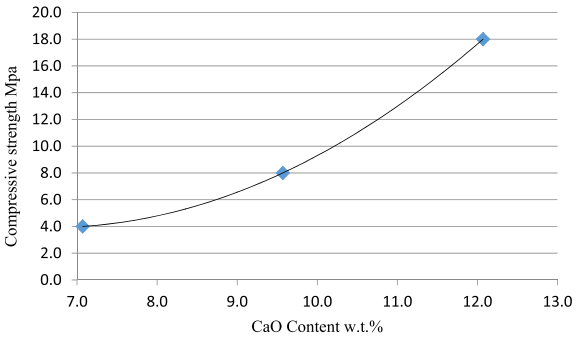

Fig. 6. Compressive Strength of the set cements as a function of CaO content.

was added as phosphoric acid to the milled powder and mixed with a spatula. The mix is enclosed in a sealed nylon bag and kept for one week at a local ambient temperature (≈35 °C). After that, the powder was dried in an oven for 2 h at 120 °C. Finally, The AlF_3 and CaF were added to the powder. Each batch, with different CaF content, is melted at 900 °C for 30 min and quenched in the air; then crashed and re-melted to ensure homogeneity. The final patches were again crushed and milled for 6 h via a high-speed grinder.

The particle size of the final fluoroaluminosilicate powders was measured via (NanoBrook 90Plus Particle Size Analyzer, New York, USA) and it was 235 ± 15 nm. The cement powder was prepared by mixing each of the prepared fluoroaluminosilicate powder with 20 w.t.% polyacrylic acid similar to SDI-Riva Luting GIC [32]. The liquid part of the same

Table 3
The working and setting times of the prepared cements.

Batch	w.t. fraction of the fluorapatite in the set cement	w.t.	s.t.
#1	0.20	37	180
#2	0.25	76	210
#3	0.27	92	230

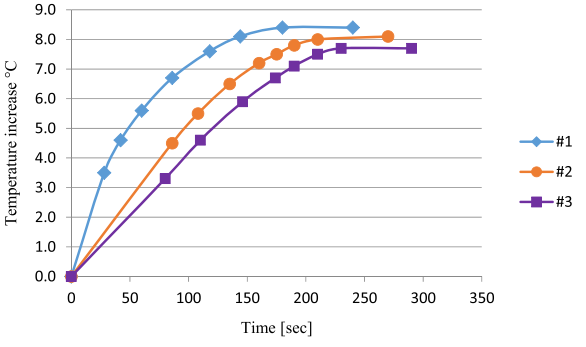

Fig. 7. The temperature rise of the cements during the setting reaction.

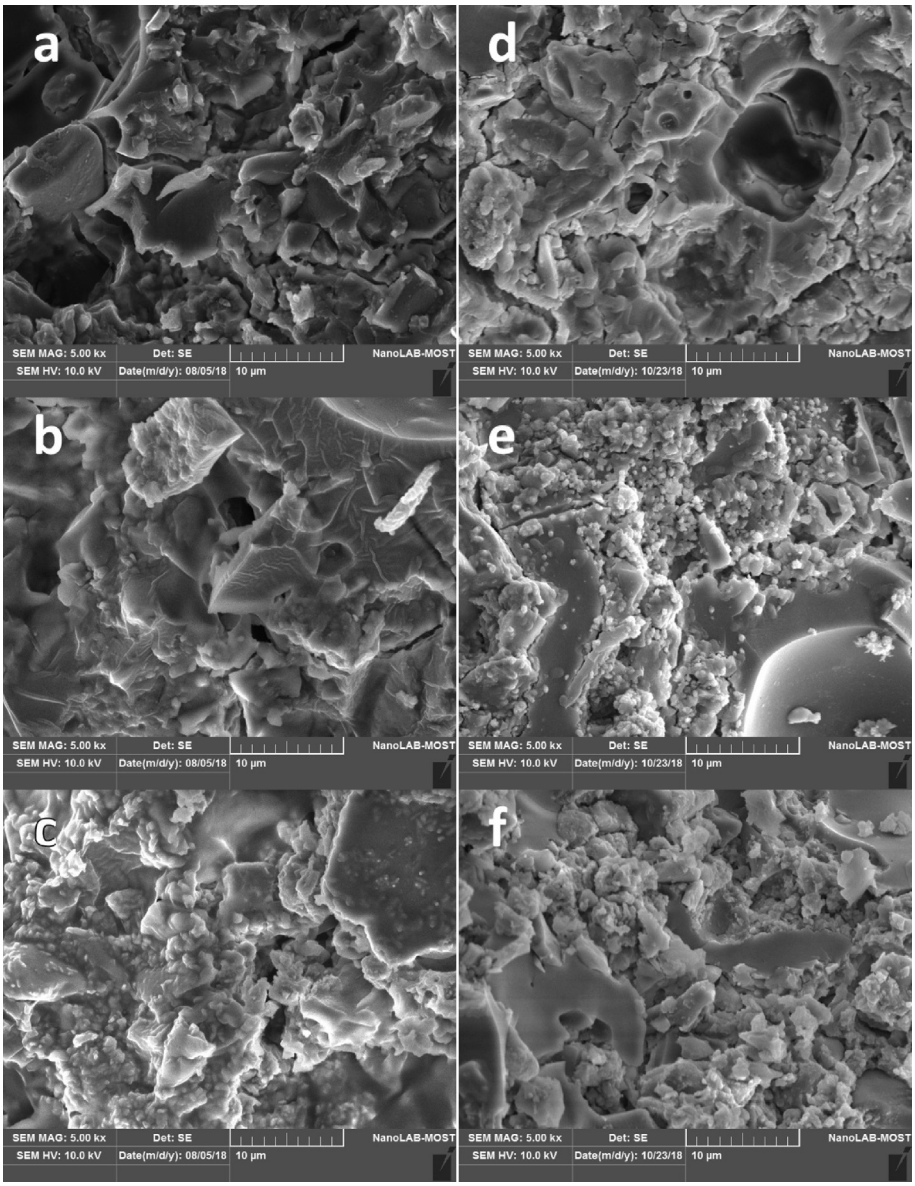

Fig. 8. SEM micrographs for the fracture surfaces of the set cements. (a), (b), (c): for cement #1, #2, and #3 respectively before exposure to SBF solution. (d), (e), (f): after exposure to SBF solution for one week.

product was utilized for the setting of the cement; which is an aqueous solution with 15 w.t.% of polyacrylic acid and 10 w.t.% of tartaric acid [33]. The set cements were given the same batch numbers of the originated fluoroaluminosilicate glass. The working and setting times were measured following ADA protocol [34], which depends on the rise of the temperature of the cement throughout the setting reaction until reaching a plateau. According to ADA protocol, the time of the start of the temperature plateau is the setting time and the time at which the temperature increase is half of that of the plateau is the working time. The powder/liquid p/l ratio that gave the max working times is 2 g/g and thus, it was fixed throughout the experimental work. In addition, the densities of the set cements were measured according to ASTM C373-88 [35].

X-ray diffraction (Cu-$k_{\alpha 1}$) for the fluoroaluminosilicate powders and the set cements were performed via Shimadzu XRD 6000 (Japan). SEM micrographs were obtained for the fracture surfaces of the set cements using TESCAN VEGA3 (Czech

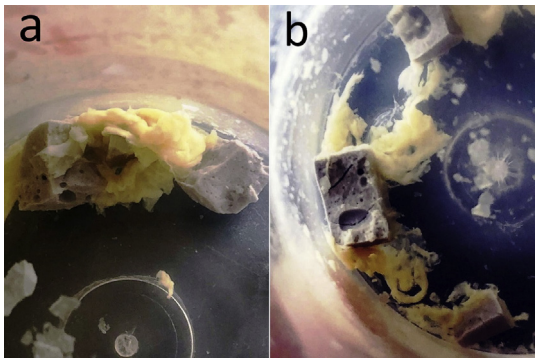

Fig. 9. The set cement samples dipped in SBF solution for one week, a, b. A precipitate has appeared in the vicinity of the samples.

Republic). The examined fracture surfaces were before and after exposure to Simulated Body Fluid (SBF) solution for one week to check for bioactivity as well be explained in the next section. The compressive strengths for the set cements were measured via (Laryee universal testing machine, China) according to ASTM C1424-99 [36].

3. Results and discussion

The x-ray diffraction results showed that the prepared fluoroaluminosilicate glass powders were fully amorphous. Fig. 1 is a representative XRD for the prepared glasses. On the other hand, the XRD of the set cements has shown both the amorphous character and the crystalline characters as seen in Figs. 2–4. The crystalline phase was analyzed for each type of the set cement and found that the crystalline phase was merely fluorapatite $Ca_5(PO_4)_3F$ that match JCPDF #15-0876. Accordingly, the bioactivity of the set cement is expected. In simple terms, the bioactivity of an implant is its ability to enhance the growth of the bone tissue via dissolution to, or, leaching apatite like molecules when exposed to the living body fluid. Immersion in SBF is a usual check for the release of apatite like molecules. The reported immersion times were different in literature, however, immersion time of one week is very frequent [37–39]. In this study, the leached apatite like molecules was the fluorapatite, which was obvious after one week of immersion.

The density for each set cement is shown in Fig. 5 as a function of CaO content. The density was increased with increasing CaO content. This may be attributed to the increase of the crystalline content, the fluorapatite, with increasing CaO content. The density of the fluorapatite is 3.201 g cm^{-1}. Thus, with the aid of the fitting equation in Fig. 5, the w.t. a fraction of the fluorapatite for each of the set cements #1, #2, and #3 was as shown in Table 3. However, the small variation of the w. t. a fraction of the fluorapatite led to a noticeable difference in the compressive strengths of the set cement as shown in Fig. 6. The higher compressive strength of the higher CaO content may be attributed to the higher packing of the microstructure as indicated by the higher density.

The rise in temperature of the cement during the setting reaction is shown in Fig. 7. The curves resemble monotonic increase and slowed down to reach plateaus. The working and setting times, according to ADA protocol, described above, are shown in Table 3 for each of the prepared cement. The working time noticeably increased with the increase of

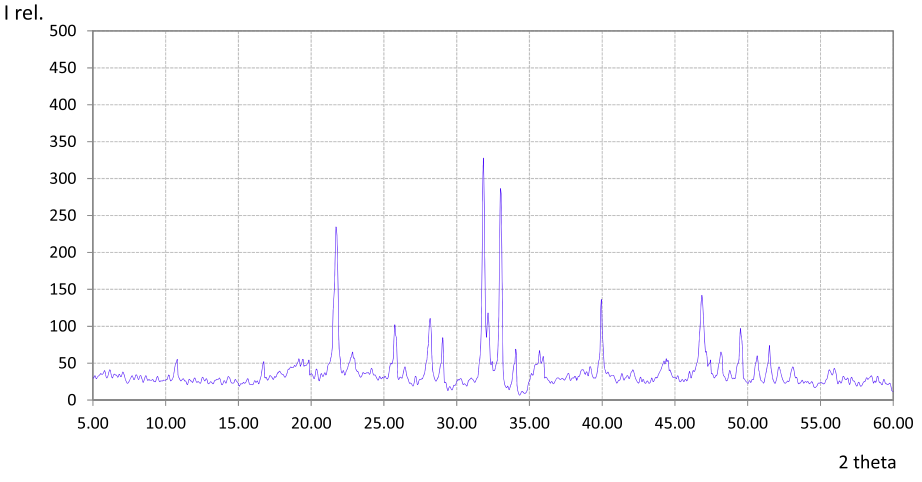

Fig. 10. X-ray diffraction pattern of the dried precipitate shown in Fig. 9.

the w.t. fraction of the fluorapatite. However, the setting time also increases together with the working time but it does not exceed 4 min. The increase in the working time is useful because it gives more flexibility to the dentist to manipulate the cement to the desired shape and quantity.

Fig. 8 shows SEM micrographs for the fracture surfaces of the set cements before and after exposure to the SBF solution. For the set cements before exposure to SBF, #1, #2, and #3 shown in part a, b, c; it appears the grain sizes increases in sequence, i.e. the grain sizes increase with increasing the CaO content. In other words, the grain sizes increase with the increase of the crystalline fluorapatite content. This result is understood in terms of that the crystalline phase is harder to solve by the polyacrylic acid than the glass phase. After exposure to SBF solution, Fig. 8 d, e, f; the microstructure for each cement did not appear to vary substantially. However, a careful look at the micrographs may reveal that a new phase (an apatite) may partially fill the voids of the microstructure. Fig. 9 shows the fractured cements samples dipped in SBF solution for one week. After that, a precipitate has appeared in the solution as a result of leaching from the fractured samples. An amount of the precipitate was collected and dried. The XRD of the dried precipitate, Fig. 10, shows that it was again fluorapatite. Thus, the new phase shown in Fig. 8 d, e, f; is strongly suggested as fluorapatite. This result may support that the prepared cements were bioactive [39,40].

4. Conclusion

Low-cost glass ionomer cements were prepared starting from a recycled low alumina glass. AlF_3, CaF, and H_3PO_4 were added to produce the fluoroaluminosilicate glass as the core solid part of the cement. The densities, compressive strengths, working and setting times were increased with increasing CaO content. In addition, the set cements were shown bioactive.

References

[1] S. Sidhu, J. Nicholson, A review of glass-ionomer cements for clinical dentistry, J. Funct. Biomater. 7 (2016) 16, https://doi.org/10.3390/jfb7030016.

[2] M.F. Burrow, Physicochemical nature of glass-ionomer-based materials and their clinical performance. Glass-Ionomers in Dentistry, Springer, 2016, pp. 25−56.

[3] J.W. Nicholson, Adhesion of glass-ionomer cements to teeth: a review, Int. J. Adhesion Adhes. 69 (2016) 33−38, https://doi.org/10.1016/j.ijadhadh.2016.03.012.

[4] S. Shahid, T. Duminis, Glass-ionomer cement: chemistry and its applications in dentistry. Advanced Dental Biomaterials, Elsevier, 2019, pp. 175−195.

[5] S.G. Griffin, R.G. Hill, Influence of glass composition on the properties of glass polyalkenoate cements. Part I: influence of aluminium to silicon ratio, Biomaterials 20 (1999) 1579−1586, https://doi.org/10.1016/S0142-9612(99)00058-7.

[6] S.G. Griffin, R.G. Hill, Influence of glass composition on the properties of glass polyalkenoate cements. Part II: influence of phosphate content, Biomaterials 21 (2000) 399−403, https://doi.org/10.1016/S0142-9612(99)00202-1.

[7] E. De Barra, R.G. Hill, Influence of glass composition on the properties of glass polyalkenoate cements. Part III: influence of fluorite content, Biomaterials 21 (2000) 563−569, https://doi.org/10.1016/S0142-9612(99)00215-X.

[8] S.G. Griffin, R.G. Hill, Influence of glass composition on the properties of glass polyalkenoate cements. Part IV: influence of fluorine content, Biomaterials 21 (2000) 693−698, https://doi.org/10.1016/S0142-9612(99)00216-1.

[9] A. Stamboulis, F. Wang, Ionomer glasses: design and characterization. Advanced Biomaterials, John Wiley & Sons, Ltd, 2010, pp. 411−433. https://onlinelibrary.wiley.com/doi/abs/10.1002/9780470891315.ch12.

[10] A. Debnath, S.B. Kesavappa, G.P. Singh, S. Eshwar, V. Jain, M. Swamy, P. Shetty, Comparative evaluation of antibacterial and adhesive properties of chitosan modified glass ionomer cement and conventional glass ionomer cement: an in vitro study, J. Clin. Diagn. Res. 11 (2017) ZC75, https://doi.org/10.7860/JCDR/2017/25927.9593.

[11] M.A. Fareed, A. Stamboulis, Nanoclays reinforced glass ionomer cements: dispersion and interaction of polymer grade (PG) montmorillonite with poly (acrylic acid), J. Mater. Sci. Mater. Med. 25 (2014) 91−99, https://doi.org/10.1007/s10856-013-5058-3.

[12] M.A. Fareed, A. Stamboulis, Nanoclay addition to a conventional glass ionomer cements: influence on physical properties, Eur. J. Dermatol. 8 (2014) 456, https://doi.org/10.4103/1305-7456.143619.

[13] V.P. Chalissery, N. Marwah, M. Almuhaiza, A.M. AlZailai, E.P. Chalisserry, S.H. Bhandi, S. Anil, Study of the mechanical properties of the novel zirconia-reinforced glass ionomer cement, J. Contemp. Dent. Pract. 17 (2016) 394−398, https://doi.org/10.5005/jp-journals-10024-1861.

[14] J.C. Souza, J.B. Silva, A. Aladim, O. Carvalho, R.M. Nascimento, F.S. Silva, A.E. Martinelli, B. Henriques, Effect of zirconia and alumina fillers on the microstructure and mechanical strength of dental glass ionomer cements, Open Dent. J. 10 (2016) 58, https://doi.org/10.2174/1874210601610010058.

[15] S. Najeeb, Z. Khurshid, M. Zafar, A. Khan, S. Zohaib, J. Martí, S. Sauro, J. Matinlinna, I. Rehman, Modifications in glass ionomer cements: nano-sized fillers and bioactive nanoceramics, Int. J. Mol. Sci. 17 (2016) 1134, https://doi.org/10.3390/ijms17071134.

[16] I.A. Moheet, N. Luddin, I. Ab Rahman, T.P. Kannan, N.R.N.A. Ghani, Evaluation of mechanical properties and bond strength of nano-hydroxyapatite-silica added glass ionomer cement, Ceram. Int. 44 (2018) 9899−9906, https://doi.org/10.1016/j.ceramint.2018.03.010.

[17] R.A. Alatawi, N.H. Elsayed, W.S. Mohamed, Influence of hydroxyapatite nanoparticles on the properties of glass

ionomer cement, J. Mater. Res. Technol. 8 (2019) 344−349, https://doi.org/10.1016/j.jmrt.2018.01.010.

[18] M. Kheur, N. Kantharia, T. Iakha, S. Kheur, N.A.-H. Husain, M. Özcan, Evaluation of mechanical and adhesion properties of glass ionomer cement incorporating nano-sized hydroxyapatite particles, Odontology (2019) 1−8, https://doi.org/10.1007/s10266-019-00427-5.

[19] A.Z. Karimi, E. Rezabeigi, R.A. Drew, Glass ionomer cements with enhanced mechanical and remineralizing properties containing 45S5 bioglass-ceramic particles, J. Mech. Behav. Biomed. Mater. 97 (2019) 396−405, https://doi.org/10.1016/j.jmbbm.2019.05.033.

[20] D.D. Cibim, M.T. Saito, P.A. Giovani, A.F.S. Borges, V.G.A. Pecorari, O.P. Gomes, P.N. Lisboa-Filho, F.H. Nociti-Junior, R.M. Puppin-Rontani, K.R. Kantovitz, Novel nanotechnology of TiO2 improves physical-chemical and biological properties of glass ionomer cement, Int. J. Biomater. 2017 (2017), https://doi.org/10.1155/2017/7123919.

[21] S.K. Garoushi, J. He, P.K. Vallittu, L.V. Lassila, Effect of discontinuous glass fibers on mechanical properties of glass ionomer cement, Acta Biomater. Odontol. Scand. 4 (2018) 72−80, https://doi.org/10.1080/23337931.2018.1491798.

[22] L. Sun, Z. Yan, Y. Duan, J. Zhang, B. Liu, Improvement of the mechanical, tribological and antibacterial properties of glass ionomer cements by fluorinated graphene, Dent. Mater. 34 (2018), https://doi.org/10.1016/j.dental.2018.02.006 e115−e127.

[23] R. Menezes-Silva, B.M.B. de Oliveira, P.H.M. Fernandes, L.Y. Shimohara, F.V. Pereira, A.F.S. Borges, M.A.R. Buzalaf, R.C. Pascotto, S.K. Sidhu, M.F. de Lima Navarro, Effects of the reinforced cellulose nanocrystals on glass-ionomer cements, Dent. Mater. 35 (2019) 564−573, https://doi.org/10.1016/j.dental.2019.01.006.

[24] I.A. Moheet, N. Luddin, I. Ab Rahman, T.P. Kannan, N.R.N.A. Ghani, S.M. Masudi, Modifications of glass ionomer cement powder by addition of recently fabricated nano-fillers and their effect on the properties: a review, Eur. J. Dermatol. (2019), https://doi.org/10.1055/s-0039-1693524.

[25] D. Kim, H. Abo-Mosallam, H.-Y. Lee, J.-H. Lee, H.-W. Kim, H.-H. Lee, Biological and mechanical properties of an experimental glass-ionomer cement modified by partial replacement of CaO with MgO or ZnO, J. Appl. Oral Sci. 23 (2015) 369−375, https://doi.org/10.1590/1678-775720150035.

[26] M. Almuhaiza, Glass-ionomer cements in restorative dentistry: a critical appraisal, J. Contemp. Dent. Pract. 17 (2016) 331, https://doi.org/10.5005/jp-journals-10024-1850.

[27] H.S. Ching, N. Luddin, T.P. Kannan, I. Ab Rahman, N.R. Abdul Ghani, Modification of glass ionomer cements on their physical-mechanical and antimicrobial properties, J. Esthetic Restor. Dent. 30 (2018) 557−571, https://doi.org/10.1111/jerd.12413.

[28] A. Sajjad, W.Z.W. Bakar, D. Mohamad, T.P. Kannan, Various recent reinforcement phase incorporations and modifications in glass ionomer powder compositions: a comprehensive review, J. Int. Oral Health 10 (2018) 161, https://doi.org/10.4103/jioh.jioh_160_18.

[29] S. Najeeb, Z. Khurshid, H. Ghabbani, M.S. Zafar, F. Sefat, Nano glass ionomer cement: modification for biodental applications. Advanced Dental Biomaterials, Elsevier, 2019, pp. 217−227.

[30] N. Alvanforoush, R. Wong, M. Burrow, J. Palamara, Fracture toughness of glass ionomers measured with two different methods, J. Mech. Behav. Biomed. Mater. 90 (2019) 208−216, https://doi.org/10.1016/j.jmbbm.2018.09.020.

[31] R. Menezes-Silva, R.N. Cabral, R.C. Pascotto, A.F.S. Borges, C.C. Martins, M.F. de L. Navarro, S.K. Sidhu, S.C. Leal, Mechanical and optical properties of conventional restorative glass-ionomer cements-a systematic review, J. Appl. Oral Sci. 27 (2019), https://doi.org/10.1590/1678-7757-2018-0357.

[32] SDI, Material Safety Data Sheet, Product: RIVA luting (Powder), Retrieved at 2019-Aug-08, https://www.sdi.com.au/wp-content/uploads/SDS/SDS_CR_CZ/Riva%20Luting%20Powder_DS_EN.pdf.

[33] SDI, Material Safety Data Sheet, Product: RIVA Luting (Lquid), Retrieved at 2019-Aug-08, https://www.sdi.com.au/wp-content/uploads/SDS/SDS_CR_CZ/Riva%20Luting%20Liquid_DS_EN.pdf.

[34] ADA, Professional product review laboratory testing methods: core materials, Am Dent Assoc 3 (2008) 1−18. https://www.ada.org/en/publications/ada-professional-product-review-ppr/archives/2008.

[35] The American Society for Testing and Materials, Water Absorption, Bulk Density, Apparent Porosity, and Apparent Specific Gravity of Fired Whiteware Products, 2006, pp. 1−2, https://doi.org/10.1520/C0373-88R06. ASTM C373-88.

[36] The American Society for Testing and Materials, Standard Test Method for Monotonic Compressive Strength of Advanced Ceramics at Ambient Temperature, 2006, pp. 1−13, https://doi.org/10.1520/C1424-99. ASTM C1424-99.

[37] K.J. Roche, K.T. Stanton, Measurement of fluoride substitution in precipitated fluorhydroxyapatite nanoparticles, J. Fluor. Chem. 161 (2014) 102−109, https://doi.org/10.1016/j.jfluchem.2014.02.007.

[38] R. Taktak, A. Elghazel, J. Bouaziz, S. Charfi, H. Keskes, Tricalcium phosphate-Fluorapatite as bone tissue engineering: evaluation of bioactivity and biocompatibility, Mater. Sci. Eng. C. 86 (2018) 121−128, https://doi.org/10.1016/j.msec.2017.11.011.

[39] S. Manafi, F. Mirjalili, R. Reshadi, Synthesis and evaluation of the bioactivity of fluorapatite−45S5 bioactive glass nanocomposite, Prog. Biomater. 8 (2019) 77−89, https://doi.org/10.1007/s40204-019-0112-y.

[40] T. Kokubo, H. Takadama, How useful is SBF in predicting in vivo bone bioactivity? Biomaterials 27 (2006) 2907−2915, https://doi.org/10.1016/j.biomaterials.2006.01.017.